

Potentialities and criticalities of flexible-rate transponders in DWDM networks: A statistical approach

*Original*

Potentialities and criticalities of flexible-rate transponders in DWDM networks: A statistical approach / Cantono, Mattia; Gaudino, Roberto; Curri, Vittorio. - In: JOURNAL OF OPTICAL COMMUNICATIONS AND NETWORKING. - ISSN 1943-0620. - ELETTRONICO. - 8:7(2016), pp. A76-A85. [10.1364/JOCN.8.000A76]

*Availability:*

This version is available at: 11583/2652919 since: 2021-04-07T10:30:27Z

*Publisher:*

Institute of Electrical and Electronics Engineers Inc.

*Published*

DOI:10.1364/JOCN.8.000A76

*Terms of use:*

This article is made available under terms and conditions as specified in the corresponding bibliographic description in the repository

*Publisher copyright*

IEEE postprint/Author's Accepted Manuscript

©2016 IEEE. Personal use of this material is permitted. Permission from IEEE must be obtained for all other uses, in any current or future media, including reprinting/republishing this material for advertising or promotional purposes, creating new collecting works, for resale or lists, or reuse of any copyrighted component of this work in other works.

(Article begins on next page)

# Potentialities and Criticalities of Flexible-Rate Transponders in DWDM networks: a Statistical Approach

Mattia Cantono, *Student Member, IEEE*, Roberto Gaudino, *Senior Member, IEEE*,  
and Vittorio Curri, *Member, IEEE*

**Abstract**—We propose a novel method to assess physical layer potentialities of core optical networks aimed at finding solutions better exploiting the installed equipment. We focus on the use of flexible-rate transponders for the implementation of the elastic paradigm on the state-of-the-art DWDM – fixed-grid – network scenarios. We make use of the waveplane-based routing and wavelength assignment (RWA) algorithm presented in [pippo] to implement a progressive statistical loading of the analyzed network topology, and perform a Monte Carlo analysis delivering a statistical characterization of the average bit-rate per lightpath together with the assessment of network blocking. The proposed method allows identifying criticalities in terms of link congestion and lightpath quality of transmission, addressing solutions by identifying network bottlenecks. We apply the proposed method to a large Pan-European network topology comparing two different transmission techniques for the implementations of flexible-rate transponders: *pure* PM-m-QAM vs. hybrid modulation formats. Over this realistic network example, besides displaying the overall statistics for the average bit-rate per lightpath, we show statistics for critical lightpaths and congested fiber links.

**Index Terms**—Optical Fiber Networks, Waveplane-based network performance analysis, optical fiber communications.

## I. INTRODUCTION

THE IP traffic is foreseen to grow at a compound annual growth-rate (CAGR) of 23% from 2014 to 2019 [1], roughly corresponding to a 2.8 fold growth in 5 years. According to [1], the increase of traffic generated by the final user will become dominant in the analyzed period 2014-2019, thanks to the diffusion of personal applications sharing data – mostly videos – on the Internet, enabled by the pervasive diffusion of broadband access technologies. Moreover, the traffic for the 60 busiest minutes of the day will experience a growth rate 20% higher than the average internet traffic.

A similar scenario will strongly modify the traffic model for core transport networks, which will become more and more unpredictable and subjected to serious variations with time. Therefore, such networks – besides growing as total transport capacity – will have to be responsive to relevant dynamic fluctuations of traffic demand. Hence, the implementation of the elastic network paradigm will be a firm and unpostponable request.

On the other hand, it should be considered that large telecommunications carriers intend to continue exploiting the

already installed fibers roughly until 2025 [2]. Such a requirement is aimed at returning from large CAPEX investments on fiber links done at the beginning of year 2000s [2]. Hence, core network operators are looking for solutions allowing to maximize the aggregate bit-rate on the already used fiber links thanks to advanced modulation formats and coherent detection, enabling at the same time flexible network loading. First, they will optimize Dense Wavelength Division Multiplexed (DWDM) fixed grid transmission with the newest and most performing flexible transponders being able to trade-off the delivered data-rate with the quality of transmission of the available lightpath. Then, after reaching a capacity saturation on active fibers, they will start to selectively switch on available single mode dark fibers, by planning spatial-division multiplexing (SDM), avoiding for the envisioned time-span the installation of SDM solutions based on multicore or multimode fibers. To pursue such results, an accurate assessment of potentialities and criticalities of network physical layer is an indispensable request.

As the use of elastic transponders is a key technology for the implementation of the elastic paradigm in DWDM networks [3], in this paper we compare two different implementations of flexible transponders based on polarization-division-multiplexed (PM) M-QAM modulation formats. One transponders' family able to switch between M-QAM constellations – *pure* formats – delivering quantized bit-rate values. The other considers the use of time-division hybrid modulation formats (TDHMF) [4], [5] enabling to tune with continuity the bit-rate, tailoring its value to the lightpath's (LP) optical signal-to-noise ratio (OSNR). A more detailed description of these technologies can be found in [4]–[6].

To perform the aforementioned comparison, we propose an innovative approach that we call Statistical Network Assessment Process (SNAP). This methodology starts from the waveplane-based routing and wavelength assignment (RWA) [6], [7] and performs a progressive load of the network through a Monte Carlo analysis [8] in which the order according to which lightpath demands are served is varied. SNAP applies to both static and dynamic traffic models and in this paper, it is used for a static traffic scenario, i.e. with demands of infinite duration. The core concept of this method is to analyze a progressive random load of traffic to an optical network, and to evaluate its performance under such random traffic conditions. The network can be completely unloaded at the beginning of the process – as it is in this work – or can carry

The authors are with the Department of Electronics and Telecommunications, Politecnico di Torino, Torino, Italy. Website: [www.optcom.polito.it](http://www.optcom.polito.it)  
e-mail: [mattia.cantono@polito.it](mailto:mattia.cantono@polito.it)

some existing traffic. In our analysis we consider networks operating according to the LOGO optimization strategy [9], [10], meaning that each link runs at its optimal power [11], [12]. Given the network topology graph, each fiber link is weighted by a quality of transmission (QoT) metric – the Optical *Noise-to-Signal* Ratio accumulation – computed by means of the incoherent GN-Model [11]. This QoT cost is used during the network loading phase for routing purposes, and to determine the maximum bit-rate at which each lightpath can operate for a given modulation strategy. Operating on a detailed description of the network topology, SNAP is able to estimate the statistics of the average bit-rate per lightpath  $R_{b,\lambda}$  for all possible lightpath demands' arrangement. It also evaluates the network blocking performances, defined here as the ratio between the number of blocked demands over the total number of lightpath demands. Moreover, it statistically determines the criticalities of the physical layer, as, for instance, the congestion of node-to-node links or the critical QoT in lightpaths. Such statistical characterization of critical aspects can be fruitfully used to derive general and statistically effective solutions. The knowledge of the full statistics of network metrics leads to understanding useful insights on network performances. For example, the statistics of the average bit-rate per LP, obtained through SNAP, can be used to assess the goodness of heuristics algorithms aimed at throughput maximization. In particular, one could easily state in which percentile of the distribution, the average bit-rate per LP obtained with the considered heuristics falls. In addition to this, one could also assess statistically network striking features. For example, using SNAP may deliver the probability for the spectrum of a link to be utilized over a certain percentage, given some traffic, RWA, topology and physical layer characteristics. Although Monte Carlo based algorithms for network analysis have been frequently used in the past [6], [13], [14], the statistical interpretation of network metrics is a novel approach, to the best of our knowledge.

We remark that the proposed method is not aimed at providing optimal routing and wavelength solutions for a given traffic matrix and network topology, instead, it addresses the statistical benchmarking of the physical layer on a re-configurable optical network scenario to identify its strengths and weaknesses under a random progressive traffic load.

Using SNAP, we compare the two considered flexible-rate transponder technologies on a Pan-European network topology. We show that TDHMFs enable a capacity enhancement of 23% at a target pre-FEC Bit Error Rate (BER) level of  $4 \cdot 10^{-3}$  with respect to *pure* formats, independently on the characteristic of the Routing and Wavelength Assignment (RWA) algorithm considered in this paper. Moreover, we prove the importance of correctly modeling non-linear fiber propagation to properly estimate network performances. In particular, we consider as non-linear propagation effect the generation of a noise-like disturbance called non-linear interference (NLI) [11], [15]–[23].

On the analyzed topology, we also show detailed results on links' congestion and suggest possible general remedies to these criticalities.

The paper is organized as follows. Sec. II is devoted to

describing the SNAP algorithm. Sec. III shows the use of SNAP to perform the comparison between pure and hybrid modulation approaches. In Sec. IV the Pan-European network scenario chosen for the comparison is described. Finally, in Sec. V results are shown and commented, and in Sec. VI conclusions are made.

## II. SNAP: STATISTICAL NETWORK ASSESSMENT PROCESS

In this section, we introduce the Statistical Network Assessment Process (SNAP). SNAP is an algorithm to statistically characterize the strengths and weaknesses of the physical layer in re-configurable optical networks, and it is here applied to compare hybrid to pure modulation strategies for the implementation of flexible-rate transponders.

In this paper, we use the following network terminology. We refer to lightpaths as transparent optical connections between nodes not directly connected by fiber links. We suppose that network nodes include the equipment responsible for traffic loading and retrieving and for transparent wavelength routing. Optical amplification at each output port of each node is included to recover for the loss experienced by lightpaths transparently routed, and to set the optimal power per channel on the output link. We define fiber links as connections between two nodes. Fibers between nodes are in pairs, providing bidirectional connectivity between the nodes such that the network is considered as an undirected graph. Each fiber link is made by a cascade of identical spans. Each span is made of fiber followed by an Erbium Doped Fiber Amplifier (EDFA) fully recovering its loss.

The flow chart of Fig. 1 describes the proposed algorithm. SNAP makes use of the following input information:

- 1) A set of node-to-node lightpaths' demands organized in a matrix fashion. Each element of the matrix  $D_{i,j}$  represents the number of lightpaths to be allocated between node  $i$  and node  $j$ . While SNAP can work with any  $D_{i,j}$  matrix, in Sec. IV we will focus on  $D_{i,j} = 1 \forall i, j$  and  $D_{i,j} = 0$  for  $i = j$ , i.e., one lightpath request for each node pair. Since we aim at analyzing the potentialities of the physical layer of a fully re-configurable optical network, we consider demands expressed in terms of number of requested lightpaths' and not as data-rate.
- 2) A full description of the network topology and the characteristics of the physical layer (e.g., fiber type, amplification method, slot size, number of channels, etc.). The physical layer parameters can be used to compute the figure of merit for the Quality-of-Transmission (QoT) of each lightpath, i.e., its Optical Signal-to-Noise Ratio (OSNR). To do so, several non-linear propagation models can be used, e.g., [11], [15]–[23]. As it will be described later on, in our analysis we exploit the incoherent Gaussian Noise (GN) model [11].
- 3) The characteristics of the Routing and Wavelength Assignment algorithm, such as the routing policy, namely the way in which fiber paths between nodes' pairs are computed and ranked. For example, a shortest link or smallest number of hops ranking could be adopted.

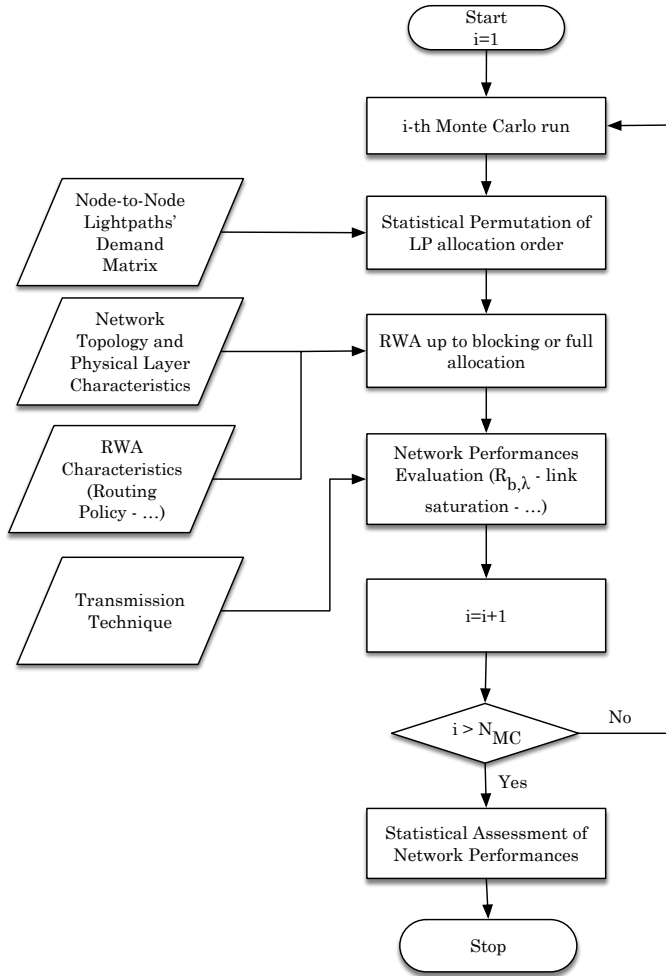


Fig. 1. Flowchart of the SNAP algorithm.

- 4) The transmission technique (e.g., pure or hybrid modulation formats) to determine the maximum allowable bit-rate of each LP given its OSNR and the related pre-FEC target BER.

Given this information, a Monte Carlo analysis is performed. During each Monte Carlo run a progressive load of the network takes place: the set of node-to-node lightpaths' demands is randomly shuffled to vary the order in which requests are allocated. It should be highlighted that in general, such progressive network load can be executed on top of any existing network loading status. In this paper, we consider a fully unloaded network. In each Monte Carlo run, given the randomly ordered list of connection, an RWA process starts. The RWA process tries to allocate each LP request according to some user-defined policies (e.g., the routing strategy). To do so, optically transparent paths able to accommodate the considered LP demands are searched across the network. In our analysis, we make use of an RWA based on the waveplane method [6], [7] that will be fully described in Sec. III, but, in general, any RWA can be used. The RWA process terminates when the complete set of demands has been considered. Depending on the traffic and network topology characteristics, the RWA process may successfully allocate all demands, or

some network blocking may occur.

After the completion of the allocation process, several network performance metrics are computed for the  $i$ -th Monte Carlo run. These may include:

- The average bit-rate per lightpath  $R_{b,\lambda}^i$  that is given by

$$R_{b,\lambda}^i = \frac{1}{N_{L,i}} \sum_{j=1}^{N_{L,i}} R_{b,j} \quad [\text{Gbps}] \quad (1)$$

where  $N_{L,i}$  is the number of allocated lightpaths during the  $i$ -th Monte Carlo run and  $R_{b,j}$  is the bit-rate of the  $j$ -th LP.

- The spectral saturation of each fiber link, i.e., the details about channel occupation of each node-to-node fiber connection.
- Blocking information such as the number of blocked demands for each node or link.

The set of metrics to be considered can be modified in order to target specific alternative network aspects. In this sense, SNAP can be easily extended providing a relevant flexibility in the characterization process. Due to the random scrambling of the set of input LPs' demands, the allocation process of each Monte Carlo run may differ from the one of the previous runs, thus, the output results of each run will be – in general – stochastic.

After the maximum number of Monte Carlo iterations  $N_{MC}$  has been reached, each metric can be statistically characterized with respect to the random allocation process of LPs. This means that the probability density function (PDF) of each analyzed metric can be derived, thus obtaining a *statistical* insight on network capabilities and critical aspects.

### III. PHYSICAL IMPAIRMENT MODEL AND ROUTING STRATEGIES

This section gives a detailed description of the non-linear modeling and RWA options adopted in this paper.

In order to compare performances of time-division hybrid and pure modulation formats in a fixed-grid network scenario, the SNAP algorithm has been properly customized. In particular, we use the incoherent GN model [11] to evaluate propagation performances, and a modified waveplane method [6], [7] with QoT-based routing to perform RWA. The incoherent GN model, is suitable for impairment-aware networking scenarios, thanks to its independence from modulation formats, and its modest computational cost. It has, however, some limitations – e.g., for low loss spans – but in general it has been proven to be sufficiently reliable for networking studies [8].

A fully transparent optical network with uniform links in terms of fiber and EDFAs types has been assumed. We consider each node to be equipped with a colorless, directionless and contentionless (CDC) re-configurable optical add-drop multiplexers (ROADMs) [24]–[26]. Each fiber span is assumed to operate at its optimal power that is computed by means of the incoherent GN model as the Locally-Optimized-Globally-Optimized (LOGO) principle prescribes [9], [10], assuming full spectral load in each link. Moreover, all node-to-node links are supposed to be made by a cascade of amplified

fiber spans. Consequently, the network may be represented as an undirected graph whose edges – the fiber links – are weighted by inverse OSNR (IOSNR) accumulation –  $\Delta_{\text{IOSNR}}$  – that includes both the amplified spontaneous emission (ASE) noise introduced by the amplifiers and the NLI disturbance by the fiber propagation. We consider as reference bandwidth for the OSNR the LP bandwidth  $B_{\text{ch}}$ .  $\Delta_{\text{IOSNR}}$  is additive span-by-span and can be computed by means of the incoherent GN-model [11]. In particular,

$$\Delta_{\text{IOSNR}} = \frac{P_{\text{ASE}}}{P_{\text{ch}}} + \eta P_{\text{ch}}^2 \quad (2)$$

where  $P_{\text{ASE}}$  is the ASE noise power in  $B_{\text{ch}}$ , while  $P_{\text{ch}}$  is the power per channel, whose optimal value is given by

$$P_{\text{ch,opt}} = \sqrt[3]{\frac{P_{\text{ASE}}}{2\eta}}. \quad (3)$$

$\eta$  is the so-called NLI efficiency and depends on fiber parameters, total occupied bandwidth  $B_{\text{opt}}$ , number of channels  $N_{\text{ch}}$ , channel bandwidth  $B_{\text{ch}}$  and the DWDM spacing  $\Delta f$ . We consider  $\eta$  in its worst case, i.e., for the center wavelength and referring to full spectral load. Such assumption is reasonable and does not cause large overestimation in links QoT due to the weak dependence between  $\eta$  and the occupied bandwidth. Interested readers may refer to [8], [10]–[12] for further details.

Given the IOSNR degradation introduced by each fiber span, it is possible to compute the OSNR of a lightpath propagating over  $N_f$  fiber links, with the  $j$ -th link made of  $N_{s,j}$  uniform spans, each of which introduces an IOSNR increase – degradation –  $\Delta_{\text{IOSNR},j}$  by considering :

$$\text{OSNR}_{\text{TOT}} = \text{IOSNR}_{\text{TOT}}^{-1} = \left[ \sum_{j=1}^{N_f} (N_{s,j} \Delta_{\text{IOSNR},j}) \right]^{-1} \quad (4)$$

Exploiting the additive property of IOSNR, it is possible to rank different lightpaths over an optical network graph based on their quality of transmission (QoT), that is directly related to the OSNR. In particular, the lightpath between two nodes having minimum  $\text{IOSNR}_{\text{TOT}}$ , will have the largest  $\text{OSNR}_{\text{TOT}}$ , hence the best QoT. Based on this, it is possible to define a QoT-based routing algorithm for optical networks, according to which lightpaths are ranked based on their QoT. The IOSNR degradation term can be used to weight edges in the optical network graph. Standard graph algorithmic techniques can be used to compute the best QoT paths between nodes' pairs. The OSNR computed by means of Eq. (4) can then be used to determine the maximum bit-rate at which a lightpath can operate given the modulation strategy (hybrid or *pure*) and the selected target BER.

As RWA strategy, we adopt a modified version of the so-called waveplane method [6] that makes use of the aforementioned QoT-based routing. The main idea of this method is to consider the network graph as a multigraph made of  $N_{\text{ch}}$  graphs, called *waveplanes*, where  $N_{\text{ch}}$  is the number of available wavelengths ( $\lambda$ s). In waveplanes, each edge of the graph corresponds to a single  $\lambda$  on the corresponding fiber link.

The waveplane-based method for RWA works as described in the following.

- 1) For each demand to be allocated, waveplanes are scanned to find a suitable working lightpath to accommodate the request.
- 2) Whenever a demand is allocated, the edges of the waveplane over which that demand was accommodated, is removed from the waveplane itself. When all links are fully saturated, all waveplanes are empty.
- 3) If a demand cannot be allocated it is flagged as blocked and the process moves to the following demand.

Differently from the original waveplane method [7], paths between a nodes' pair are computed by using a k-shortest-path algorithm, in which the best  $k_{\text{MAX}}$  paths in terms of QoT, i.e., lowest IOSNR degradation, are considered as suitable paths for LPs. In particular, the term  $k_{\text{MAX}}$  represents the number of different paths between nodes' pairs that can be used to find available wavelengths to accommodate LPs demands routes. In this sense, the adopted RWA can be classified as a first-fit wavelength assignment with routing based on a k-shortest-path, best QoT, routing policy. The use of a QoT-based routing policy allows allocating demands on the highest available QoT path between a pair of nodes, thus maximizing the bit-rate per LP, given the network loading.

We remark that the waveplane method for RWA was originally introduced as a heuristic RWA algorithm to find close-to-optimum RWA solutions for a given topology and set of traffic demands. To do so, a few randomly shuffled demand sequences are considered, and the realization which maximizes a given performance metric (e.g., the total network bit-rate) is selected as the solution of the RWA problem [6]. Within SNAP we apply it in a Monte Carlo analysis, aiming at characterizing the statistics of potentialities and criticalities of the physical layer on a re-configurable optical network scenario. Thus, we consider a much larger set of randomly shuffled sequences and we use the output of each RWA process to build the *statistics* of a set of network performance metrics of interest, to obtain results that are *independent* of the order in which LP demands are considered, thus being as general as possible.

#### IV. ANALYSIS OF THE PAN-EUROPEAN NETWORK TOPOLOGY

We tested the proposed algorithm on a realistic Pan-European network topology obtained from the EU project Idealist [27]. The considered topology has 49 nodes and 68 bidirectional fiber links and it is depicted in Fig. 2. We assume uniform links in terms of fiber and EDFA types. We consider standard single mode fiber (SMF), with the following characteristics: loss coefficient  $\alpha_{\text{dB}} = 0.2$  dB/km, dispersion coefficient  $D = 16.7$  ps/nm/km, effective area  $A_{\text{eff}} = 80 \mu\text{m}^2$ , non-linear index coefficient  $n_2 = 2.5 \cdot 10^{-20}$  m<sup>2</sup>/W corresponding to a non-linear coefficient  $\gamma = 1.27$  1/W/km. We suppose that all network ROADMs introduce a routing loss of 10 dB, that is fully recovered with an additional EDFA at the output of the nodes. We do not consider any further impairment caused by cascaded filtering effect on channel spectra caused by ROADMs. All EDFAs have a 5 dB noise

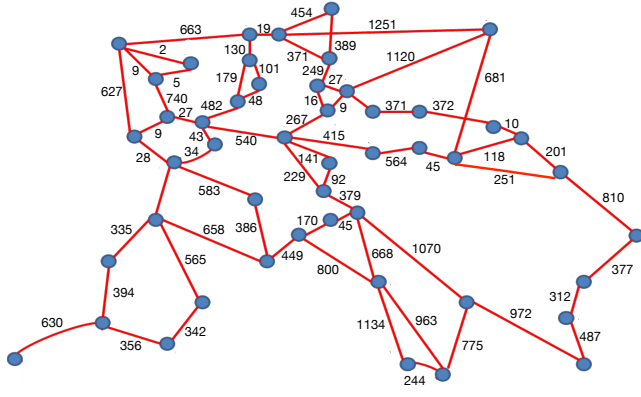


Fig. 2. Pan-European network topology. Edge labels are the lengths of each fiber pair in km.

figure. Span lengths are not uniform across the network but are given directly from the topology data obtained from [27].

We assume that the transmission level operates on the C-band set to  $B_{\text{opt}}=4$  THz and on the 50 GHz ITU-T grid, enabling a maximum of  $N_{\text{ch}} = 80$  lightpaths – wavelengths – per fiber. The network elasticity on this scenario is given by adopting flexible-rate transponders using multilevel modulation formats. We consider either elastic transponders based on pure formats – polarization multiplexed M-QAM – or on TDHMFs [4], [5]. In both cases the spectral efficiency varies from 2 to 12 Bit per Symbol (bpS), i.e., cardinality of modulation formats may adaptively grow from  $2^2$  (PM-BPSK) up to  $2^{12}$  (PM-64-QAM). However, the delivered spectral efficiency vs. the available OSNR is discrete when pure formats are used, whereas it is continuous for flexible-rate transponders based on TDHMF.

We consider modulation formats operating at gross symbol rate  $R_{s,g} = 32$  GBaud per channel, corresponding to a net symbol rate  $R_s = 25$  GBaud per channel due protocol and coding overhead. We assume that the channels operate at pre-FEC BER  $\leq 4 \cdot 10^{-3}$ . Such pre-FEC BER level is not referred to any specific standard or commercial product, as it has been selected to derive *reasonable* quantitative results. Considering specific FEC implementations, larger values of pre-FEC BER could be considered.

Firstly, we verified the convergence of the Monte Carlo analysis, i.e., the number of Monte Carlo iterations  $N_{MC}$  needed to obtain statistically stable results. To this purpose, we consider the PDF of the average bit-rate per LP given by Eq. (1) obtained with  $N_{MC} = 10^3$  and  $N_{MC} = 5 \cdot 10^4$ . Results reported in Fig. 3 are obtained considering TDHMF and selecting as feasible paths between two nodes only the path having largest OSNR, i.e.,  $k_{\text{MAX}} = 1$ .

We allocated symmetrically a single LP for each nodes' pair, i.e.,  $D_{i,j} = 1 \forall i, j$  and  $D_{i,j} = 0$  for  $i = j$ . In Fig. 3, a Gaussian fit for the two PDFs is also reported, showing good agreement with the simulative results. So, a first result of the analysis is that the average bit-rate per lightpath is Gaussian-distributed with respect to the lightpaths' allocations, and its average value can be used as figure of merit of different implementations

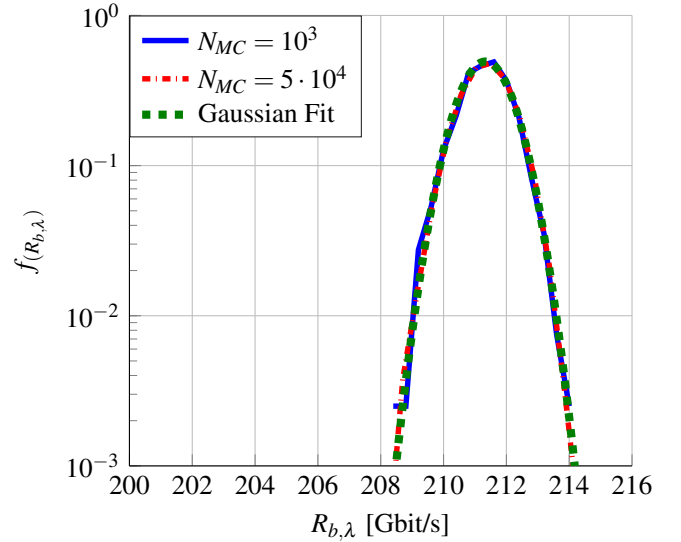


Fig. 3. Convergence of PDF of average bit-rate per LP obtained considering TDHMF and  $k_{\text{MAX}} = 1$ .

of the network physical layer. The PDF of  $R_{b,\lambda}$  converges towards a truncated Gaussian due to the central limit theorem.  $R_{b,\lambda}$  is in fact computed by summing a large set of random bit-rates, that – for TDHMF – are distributed almost uniformly in the interval [50 Gbps, 300 Gbps].

From Fig. 3 it is intuitive to understand that independently of the order in which LP demands are allocated, the considered network topology is able to deliver on average 211 Gbps per LP. This means, 4.4 bpS per polarization, that is a value larger than the one delivered by a PM-16-QAM modulation format. We also remark that the variance of  $R_{b,\lambda}$  is strictly related to the network blocking. In particular, since the complete set of LP demands cannot be allocated, the set of blocked LP demand will differ in each Monte Carlo run, so the quantity  $R_{b,\lambda}$  will be stochastic. Under the same test conditions, in particular  $k_{\text{MAX}} = 1$ , if the physical layer was able to allocate all requests, the variance of  $R_{b,\lambda}$  would be zero. This happens because all possible LP requests would be allocated on the best OSNR path, thus giving a deterministic  $R_{b,\lambda}$ . Increasing the set of feasible paths – i.e., increasing  $k_{\text{MAX}}$  – expands the variability of the overall allocation process, thus increasing the variance of  $R_{b,\lambda}$ . Thus, in general, the stochastic behavior of  $R_{b,\lambda}$  is caused by two factors: network blocking and routing strategy ( $k_{\text{MAX}} > 1$ ).

In addition to the PDF of  $R_{b,\lambda}$ , we report in Fig. 4 its mean and standard deviation – indicated as  $\langle R_{b,\lambda} \rangle$  and  $\sigma_{R_{b,\lambda}}$ , respectively – versus  $N_{MC}$ . It can be noted that the mean value of the average bit-rate per LP already converges for  $N_{MC} \geq 100$ , whereas the standard deviation converges for  $N_{MC} \geq 1000$ . Hence, in order to obtain results presented in next section we safely set  $N_{MC} = 2500$ .

## V. RESULTS AND DISCUSSION

We applied the SNAP algorithm to the Pan-European network scenario described in Sec. IV, considering the two

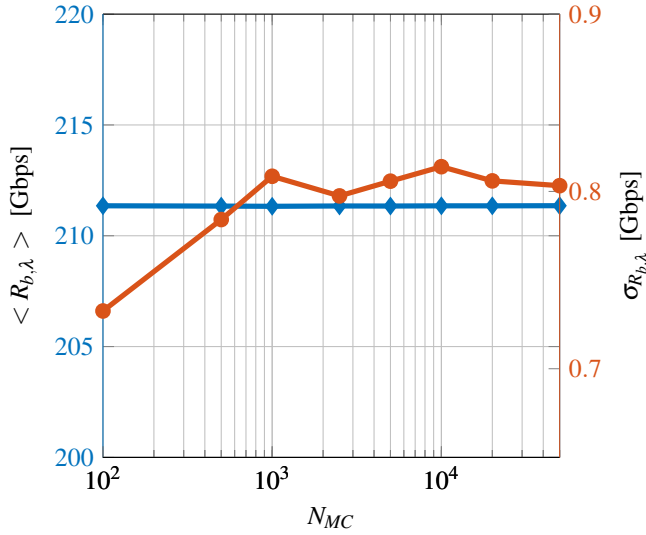


Fig. 4. Convergence of the mean value(left axis – diamond markers) and standard deviation (right axis – circular markers) of average bit-rate per LP and obtained considering TDHMF and  $k_{MAX} = 1$ .

transmission techniques operating the flexible-rate transponders described in Sec. I. The pure format approach considers elastic transponders able to select the highest cardinality squared constellation from PM-BPSK up to PM-64-QAM, thus allowing a discrete tuning in data-rate vs OSNR performances. On the other hand, TDHMF allows tuning such characteristic with continuity. For the pure format approach, we considered the formats most commonly used in coherent transceivers, i.e. the ones that are able to be used with threshold based receivers. Although flexible transceivers including PM-8-QAM can be implemented increasing the DSP complexity, we do not consider such modulation format in our study. Moreover, non-squared constellations are not uniquely defined - e.g., star-8-QAM vs. rectangle-8-QAM [28] thus introducing additional degrees of freedom to the network analysis.

As first analysis, we evaluated the impact on non-linearities on the average bit-rate per LP that the considered network can support. With such a purpose, we set the transmitted power per channel on each link  $P_{ch}$  to

$$P_{ch} = P_{ch,opt} + \Delta P \quad [\text{dBm}] \quad (5)$$

with  $\Delta P \in [-4, +4]$  dB. Each Monte Carlo analysis was performed either considering or neglecting the effect of NLI by setting  $\eta$  to zero in Eq. (2). As far as the routing policy is concerned,  $k_{MAX}$  was set to 1. Fig. 5 reports the mean value of the average bit-rate per LP  $\langle R_{b,\lambda} \rangle$  versus  $\Delta P$  for each of the two modulation strategies, both considering and neglecting NLI. The pure-format curves displays an  $\langle R_{b,\lambda} \rangle = 172$  Gbps at optimal launch power, while TDHMF allows reaching  $\langle R_{b,\lambda} \rangle = 211$  Gbps as already shown in Fig. 3, showing a 23% advantage at the selected pre-FEC BER of  $4 \cdot 10^{-3}$ . Using a more powerful FEC would probably increase the mean average bitrate per LP for both TDHMF and pure formats, but the general result, i.e. that TDHMF outperforms flex PM-m-QAM would still hold. Such noteworthy improvement is enabled by TDHMFs

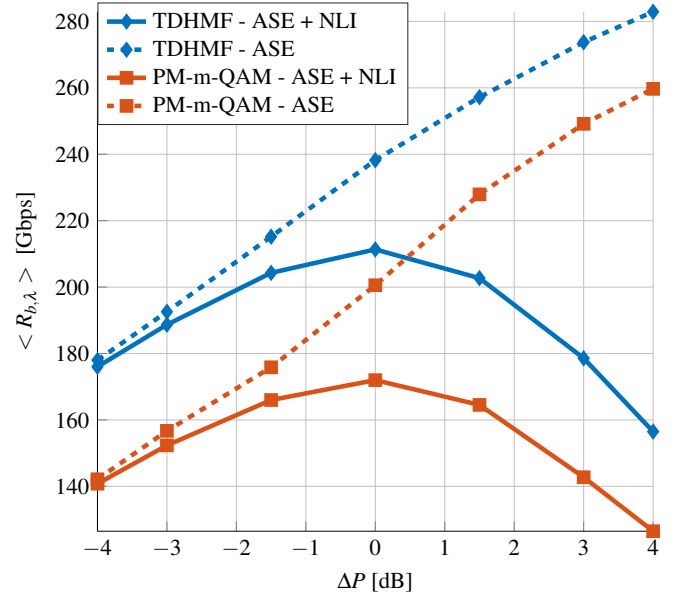


Fig. 5.  $\langle R_{b,\lambda} \rangle$  vs  $\Delta P$  for the two considered modulation strategies.  $R_{b,\lambda}$  has been averaged over  $N_{MC} = 2500$  Monte Carlo runs.

allowing a better exploitation of OSNR available on LPs, that is however traded off by an increased complexity of the Digital Signal Processing (DSP) electronics of the transceivers, thus an increased CAPEX for node equipment. Although being elastic, the pure format approach allows a poor granularity in OSNR vs. bpS, since, for instance, approximately 6 dB OSNR increase is required to move from, say, PM-QPSK to PM-16-QAM [29]. TDHMFs allow overcoming such limitation, thus supporting a relevant performance improvement at a network level.

Always referring to Fig. 5, it can be noted that neglecting NLI  $\langle R_{b,\lambda} \rangle$  is overestimated of 13% and 16% at optimal power when considering TDHMF or pure formats, respectively. In both cases the error grows up if we move away from the optimal power: 27% overestimation for TDHMF and 38% for PM-m-QAM at  $P_{ch} = P_{ch,opt} + 1$  dB.

In addition to this type of analysis, to further compare the considered modulation strategies we have estimated how varying the routing policy characteristics affects network performances. With such an objective, we have varied the parameter  $k_{MAX}$ , thus the number of ranked routes between two nodes that can be considered as suitable during the routing and allocation process of the SNAP algorithm, from 1 up to 30. As depicted in Fig. 6 a decrease in the average  $R_{b,\lambda}$  at optimal launch power and an increase in its variance take place for increasing  $k_{MAX}$ . This behavior can be explained by considering that as  $k_{MAX}$  increases, several paths with non-maximum QoT will be considered as suitable during the RWA process, thus reducing the average OSNR per LP and the corresponding average bit-rate per LP as well. Moreover, increasing  $k_{MAX}$  enlarges the set of possible paths between nodes' pairs. This provides more candidate paths for demands' allocation thus reducing the blocking ratio and expands the variability of the RWA's outcome between different Monte Carlo runs. Hence, the variance of  $R_{b,\lambda}$  increases with  $k_{MAX}$ .



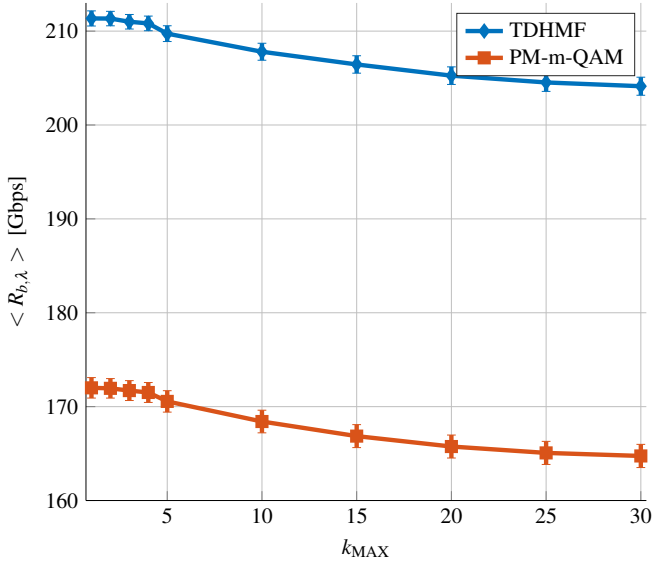


Fig. 6. Average  $R_{b,\lambda}$  vs  $k_{MAX}$  for TDHMF and PM-m-QAM modulation formats. LOGO strategy has been considered. The  $\pm\sigma$  intervals are also shown.

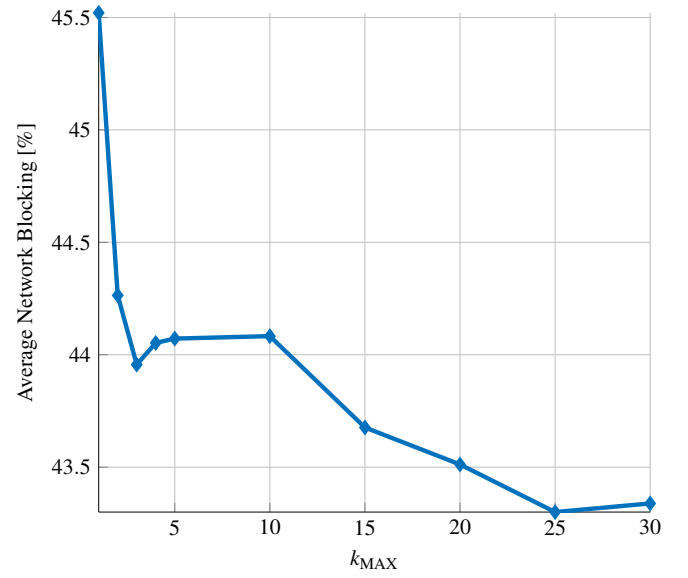


Fig. 7. Average network blocking vs  $k_{MAX}$  for TDHMF and PM-m-QAM modulation formats. LOGO strategy has been considered.

Finally, referring to Fig. 6, it can be remarked that the performance advantage of TDHMF with respect PM-m-QAM formats is independent of  $k_{MAX}$ , remaining constant around to 23%.

Finally, in order to show the capabilities of the SNAP algorithm, we report some results related to the average network blocking and link congestions, in order to highlight possible critical aspects of the considered Pan-European network topology. Fig. 7 depicts the average network blocking, i.e., the ratio between number of blocked LPs' demands and the total number of LPs' demands averaged over the set of  $N_{MC}$  of Monte Carlo runs, versus  $k_{MAX}$ . Enlarging the set of candidate paths between nodes' pairs allows to improve the number of allocated demands, but such improvement is only of the order of 2% when moving from  $k_{MAX} = 1$  to  $k_{MAX} = 30$ . This minor improvement is due to the fact that lower QoT paths between nodes' pairs share fiber links with higher QoT paths. As soon as any of these shared fiber links will be saturated, it will not be possible to allocate any additional demand on any path that will use these fiber links, losing the advantage of considering lower QoT paths.

Fig. 8 shows the average link saturation percentage of each link for each considered value of  $k_{MAX}$ . This metric is computed by considering the average over  $N_{MC}$  Monte Carlo runs, of the ratio between the number of allocated wavelengths and the total number of wavelength  $N_{ch}$  for each link of the topology. Links' indexes are sorted according to the value of the first row –  $k_{MAX} = 1$  – to improve the quality of the figure.

Fig. 9 depicts the link saturation value in the topology: the thicker the edges, the more saturated the links. Comparing Fig. 2 and Fig. 9, it can be noted that the longest links are less saturated. This is reasonable, since such links introduce larger IOSNR penalty, and therefore are not favorable from the point of view of QoT based routing. For this reason, in only a few cases long links belong to best QoT paths,

and therefore, their available wavelengths are not used. Such situation could, however, be improved by considering different RWA algorithms aimed at minimizing network blocking.

Referring to Fig. 8, it is possible to notice that many links have an average saturation that is independent of  $k_{MAX}$ . This is true especially with links with average saturation greater or equal than 60%. Less saturated links may display larger variations. Fig. 10 represents the average link saturation percentage, averaged over the set of fiber links, versus  $k_{MAX}$ . It can be noted that enlarging  $k_{MAX}$  guarantees an improvement in the average saturation of links. However, this gain is relevant up to  $k_{MAX} = 5$ , since the link saturation grows from 55% to 59%. As  $k_{MAX}$  exceeds 5, the steepness of average link saturation decreases, and the metric floors around 62%.

Thanks to Fig. 8, it is possible to identify *at a glance* all congested links, and consequently consider the option to light up available dark fiber-pairs on these links, thus planning SDM upgrades on the network. Afterward, to evaluate the benefit of the considered SDM solution – e.g., the decrease of the average network blocking – the topology can be updated to consider new fiber pairs, and the SNAP algorithm can be used once again to evaluate statistics of network performances. Fig. 8 can also be used to identify poorly used links (blue columns), and tackle inefficiencies in the RWA process. In particular, some links may be scarcely utilized due to the large IOSNR degradation that they introduce, thus being continuously discarded by the QoT based routing algorithm. Thanks to the results of SNAP algorithm these critical links can be easily recognized, and general solutions to improve this situation – e.g., the introduction of Raman amplification [30] on large  $\Delta_{IOSNR}$  links – can be once again statistically tested through SNAP. The same process can be repeated to evaluate other types of network criticalities and propose solutions to them, whose effectiveness can be evaluated statistically through SNAP.



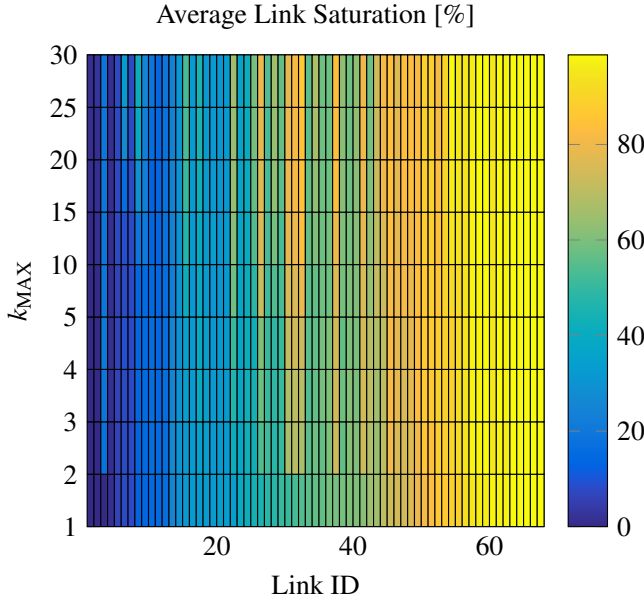


Fig. 8. Average percentage of used wavelengths for each link vs  $k_{MAX}$ .

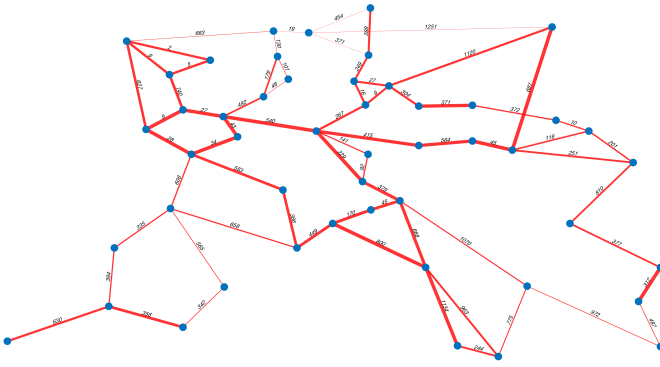


Fig. 9. Pictorial representation of link saturation in the network for  $k_{MAX} = 1$ . Ticker links correspond to more saturated links. Edge labels represent the link length in km.

## VI. COMMENTS AND CONCLUSIONS

In this paper, we carried out a comparison of flexible-rate transponders' technologies in a fixed grid network scenario. Two approaches have been considered: elastic transponders based on pure PM-m-QAM modulation formats or on TDHMFs. To perform such analysis, a novel Monte Carlo based network analysis algorithm called SNAP has been proposed and used to perform the analysis on a LOGO Pan-European network scenario. Applying SNAP, we showed that the statistics of the average bit-rate per lightpath is Gaussian-distributed with respect the lightpaths' demands and allocation. Consequently, it can be used a figure to estimate the merit of different physical layer solutions at networking level.

SNAP was also used to demonstrate the impact of NLI on maximum network performances and to show how TDHMFs outperforms pure formats, allowing a 23% improvement at

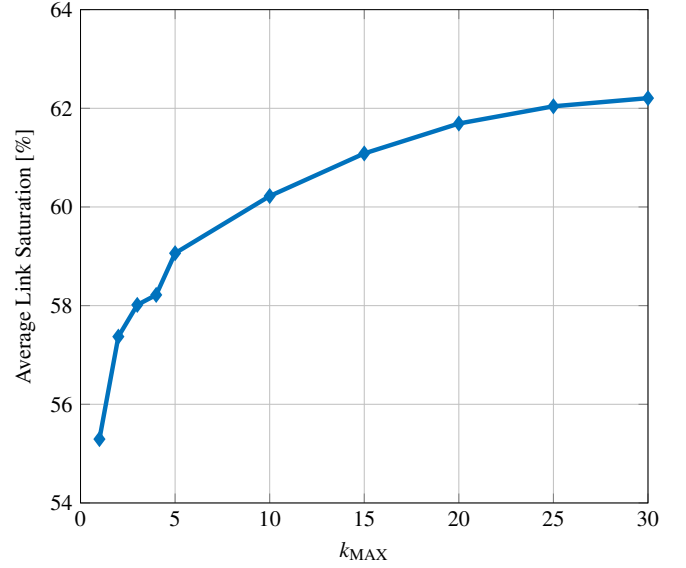


Fig. 10. Mean percentage of used wavelengths averaged over all links vs  $k_{MAX}$  for TDHMF and PM-m-QAM modulation formats. LOGO strategy has been considered.

the selected pre-FEC BER of  $4 \cdot 10^{-3}$  in terms of average bit-rate per lightpath, independently of the RWA characteristics in the considered DWDM fixed grid network. Even by using a more powerful FEC, TDHMF would still outperform PM-m-QAM, but further analyses are required to derive the exact performance gain. Showing results obtained *turning-off* the fiber non-linearities, we demonstrated how the inclusion of a detailed model for the physical layer is essential in order to properly address network performances. Possible applications of the proposed methodology have been also shown by highlighting critically congested links in the network.

Given the tight requirements imposed by network operators, the elastic paradigm will be surely implemented in various optical network technologies. Thus, we believe that further analysis will be needed in the near future to fully understand potentialities and criticalities of such technologies. In this context, the SNAP algorithm will be a useful tool for network performance assessment since it allows to precisely appraise different aspects of optical networks in a general way.

## ACKNOWLEDGMENT

The authors would like to thank M. Schiano and M. Quagliotti of Telecom Italia Lab for providing the Pan-European network model and for the helpful suggestions, Prof. E. Leonardi for the fruitful discussions, and the Reviewers for the useful comments that allowed improving the quality of this paper.

## REFERENCES

- [1] Cisco, "Cisco visual networking index: Forecast and methodology, 2014-2019," Tech. Rep., 2014.
- [2] G. Wellbrock and T. Xia, "How will optical transport deal with future network traffic growth?" in *Optical Communication (ECOC), 2014 European Conference on*, Sept 2014, pp. 1-3.
- [3] X. Zhou, L. Nelson, and P. Magill, "Rate-adaptable optics for next generation long-haul transport networks," *Communications Magazine, IEEE*, vol. 51, no. 3, pp. 41-49, March 2013.

- [4] V. Curri, A. Carena, P. Poggiolini, R. Cigliutti, F. Forghieri, C. R. Fludger, and T. Kupfer, "Time-division hybrid modulation formats: Tx operation strategies and countermeasures to nonlinear propagation," in *Optical Fiber Communication Conference*. Optical Society of America, 2014, p. Tu3A.2. [Online]. Available: <http://www.osapublishing.org/abstract.cfm?URI=OFC-2014-Tu3A.2>
- [5] F. P. Guiomar, R. Li, A. Carena, C. R. S. Fludger, and V. Curri, "Hybrid modulation formats enabling elastic fixed-grid optical networks," *submitted to IEEE/OSA Journal of Optical Communications and Networks*.
- [6] H. Dai, Y. Li, and G. Shen, "Explore maximal potential capacity of WDM optical networks using time domain hybrid modulation technique," *Lightwave Technology, Journal of*, vol. 33, no. 18, pp. 3815–3826, Sept 2015.
- [7] G. Shen, S. Bose, T. Cheng, C. Lu, and T. Chai, "Efficient heuristic algorithms for light-path routing and wavelength assignment in WDM networks under dynamically varying loads," *Computer Communications*, vol. 24, no. 3â–4, pp. 364 – 373, 2001. [Online]. Available: <http://www.sciencedirect.com/science/article/pii/S014036640000236X>
- [8] M. Cantono, R. Gaudino, and V. Curri, "Data-rate figure of merit for physical layer in fixed-grid reconfigurable optical networks," in *Optical Fiber Communication Conference*. Optical Society of America, 2016, p. Tu3F.3.
- [9] P. Poggiolini, G. Bosco, A. Carena, R. Cigliutti, V. Curri, F. Forghieri, R. Pastorelli, and S. Piciaccia, "The LOGON strategy for low-complexity control plane implementation in new-generation flexible networks," in *Optical Fiber Communication Conference/National Fiber Optic Engineers Conference 2013*. Optical Society of America, 2013, p. OW1H.3. [Online]. Available: <http://www.osapublishing.org/abstract.cfm?URI=OFC-2013-OW1H.3>
- [10] R. Pastorelli, G. Bosco, S. Piciaccia, and F. Forghieri, "Network planning strategies for next-generation flexible optical networks," *J. Opt. Commun. Netw.*, vol. 7, no. 3, pp. A511–A525, Mar 2015. [Online]. Available: <http://jocn.osa.org/abstract.cfm?URI=jocn-7-3-A511>
- [11] P. Poggiolini, G. Bosco, A. Carena, V. Curri, Y. Jiang, and F. Forghieri, "The gn-model of fiber non-linear propagation and its applications," *Lightwave Technology, Journal of*, vol. 32, no. 4, pp. 694–721, Feb 2014.
- [12] V. Curri, A. Carena, A. Arduino, G. Bosco, P. Poggiolini, A. Nespola, and F. Forghieri, "Design strategies and merit of system parameters for uniform uncompensated links supporting nyquist-wdm transmission," *J. Lightwave Technol.*, vol. 33, no. 18, pp. 3921–3932, Sep 2015. [Online]. Available: <http://jlt.osa.org/abstract.cfm?URI=jlt-33-18-3921>
- [13] L. Zhang, W. Lu, X. Zhou, and Z. Zhu, "Dynamic rmsa in spectrum-sliced elastic optical networks for high-throughput service provisioning," in *Computing, Networking and Communications (ICNC), 2013 International Conference on*, Jan 2013, pp. 380–384.
- [14] P. Wright, A. Lord, and S. Nicholas, "Comparison of optical spectrum utilization between flexgrid and fixed grid on a real network topology," in *Optical Fiber Communication Conference and Exposition (OFC/NFOEC), 2012 and the National Fiber Optic Engineers Conference*, March 2012, pp. 1–3.
- [15] A. Carena, V. Curri, G. Bosco, P. Poggiolini, and F. Forghieri, "Modeling of the Impact of Nonlinear Propagation Effects in Uncompensated Optical Coherent Transmission Links," *Lightwave Technology, Journal of*, vol. 30, no. 10, pp. 1524–1539, May 2012.
- [16] A. Bononi, P. Serena, N. Rossi, E. Grellier, and F. Vacondio, "Modeling nonlinearity in coherent transmissions with dominant intrachannel-four-wave-mixing," *Opt. Express*, vol. 20, no. 7, pp. 7777–7791, Mar 2012. [Online]. Available: <http://www.opticsexpress.org/abstract.cfm?URI=oe-20-7-7777>
- [17] A. Mecozzi and R. Essiambre, "Nonlinear Shannon Limit in Pseudo-linear Coherent Systems," *Lightwave Technology, Journal of*, vol. 30, no. 12, pp. 2011–2024, June 2012.
- [18] M. Secondini and E. Forestieri, "Analytical Fiber-Optic Channel Model in the Presence of Cross-Phase Modulation," *Photonics Technology Letters, IEEE*, vol. 24, no. 22, pp. 2016–2019, Nov 2012.
- [19] P. Johannisson and M. Karlsson, "Perturbation Analysis of Nonlinear Propagation in a Strongly Dispersive Optical Communication System," *Lightwave Technology, Journal of*, vol. 31, no. 8, pp. 1273–1282, April 2013.
- [20] R. Dar, M. Feder, A. Mecozzi, and M. Shtaif, "Properties of nonlinear noise in long, dispersion-uncompensated fiber links," *Opt. Express*, vol. 21, no. 22, pp. 25 685–25 699, Nov 2013. [Online]. Available: <http://www.opticsexpress.org/abstract.cfm?URI=oe-21-22-25685>
- [21] P. Serena and A. Bononi, "An Alternative Approach to the Gaussian Noise Model and its System Implications," *Lightwave Technology, Journal of*, vol. 31, no. 22, pp. 3489–3499, Nov 2013.
- [22] M. Secondini, E. Forestieri, and G. Prati, "Achievable Information Rate in Nonlinear WDM Fiber-Optic Systems With Arbitrary Modulation Formats and Dispersion Maps," *Lightwave Technology, Journal of*, vol. 31, no. 23, pp. 3839–3852, Dec 2013.
- [23] R. Dar, M. Feder, A. Mecozzi, and M. Shtaif, "Accumulation of nonlinear interference noise in fiber-optic systems," *Opt. Express*, vol. 22, no. 12, pp. 14 199–14 211, Jun 2014. [Online]. Available: <http://www.opticsexpress.org/abstract.cfm?URI=oe-22-12-14199>
- [24] P. Roorda and B. Collings, "Evolution to colorless and directionless ROADM architectures," in *Optical Fiber communication/National Fiber Optic Engineers Conference, 2008. OFC/NFOEC 2008. Conference on*, Feb 2008, pp. 1–3.
- [25] Y. Li, L. Gao, G. Shen, and L. Peng, "Impact of ROADM colorless, directionless, and contentionless (CDC) features on optical network performance," *Optical Communications and Networking, IEEE/OSA Journal of*, vol. 4, no. 11, pp. B58–B67, Nov 2012.
- [26] A. Devarajan, K. Sandesha, R. Gowrishankar, B. Kishore, G. Prasanna, R. Johnson, and P. Voruganti, "Colorless, directionless and contentionless multi-degree ROADM architecture for mesh optical networks," in *Communication Systems and Networks (COMSNETS), 2010 Second International Conference on*, Jan 2010, pp. 1–10.
- [27] [Online]. Available: [www.ict-ideal.eu](http://www.ict-ideal.eu)
- [28] M. Nölle, F. Frey, R. Elschner, C. Schmidt-Langhorst, A. Napoli, and C. Schubert, "Performance comparison of different 8qam constellations for the use in flexible optical networks," in *Optical Fiber Communications Conference and Exhibition (OFC), 2014, March 2014*, pp. 1–3.
- [29] D. J. Ives, P. Bayvel, and S. J. Savory, "Assessment of options for utilizing SNR margin to increase network data throughput," in *Optical Fiber Communications Conference and Exhibition (OFC), 2015, March 2015*, pp. 1–3.
- [30] V. Curri and A. Carena, "Merit of Raman pumping in uniform and uncompensated links supporting nywdm transmission," *Lightwave Technology, Journal of*, vol. PP, no. 99, pp. 1–1, 2015.